

Effect of Protonation and Zn(II) Coordination on the Fluorescence Emission of a Phenanthroline-Containing Macrocycle. An Unusual Case of “Nonemissive” Zn(II) Complex

Carla Bazzicalupi,[†] Andrea Bencini,^{*,†} Antonio Bianchi,^{*,†} Claudia Giorgi,[†] Vieri Fusi,[‡] Barbara Valtancoli,[†] M. Alexandra Bernardo,[§] and Fernando Pina^{*,§}

Department of Chemistry, University of Florence, Via Maragliano 75/77, 50144 Florence, Italy, Institute of Chemical Sciences, University of Urbino, Italy, and Departamento de Química, Centro de Química-Fina e Biotecnologia, Universidade Nova de Lisboa, Quinta da Torre 2825 Monte de Caparica, Portugal

Received December 1, 1998

Ligand 2,5,8-triaza[9]-10,23-phenanthrolinephane (**L**) contains a triamine chain connecting the 2,9 positions of a phenanthroline unit. Protonation of **L** has been studied by means of potentiometric and ¹H and ¹³C NMR techniques, allowing the determination of the basicity constants and of the stepwise protonation sites. Protonation strongly affects the fluorescence emission properties of the chemosensor **L**. The two benzylic amine groups, namely, the two aliphatic amine groups adjacent to phenanthroline, are the most efficient nitrogens in fluorescence emission quenching. In the diprotonated receptor [H₂L]²⁺ both of these nitrogens are protonated, and therefore this species is the most emissive. In the [H₃L]³⁺ species the three acidic protons are located on the amine groups of the polyamine chain. This species is still emissive, but less so than [H₂L]²⁺, due to formation of a hydrogen bond network involving the phenanthroline nitrogens, as shown by the crystal structure of the [H₃L]Br₃·H₂O salt. A potentiometric investigation of Zn(II) binding in aqueous solution suggests that some nitrogen donors are not involved, or weakly involved in metal coordination. Actually, the crystal structure of the [ZnL(H₂O)](ClO₄)₂ complex shows that both of the benzylic amine groups are weakly bound to the metal. This Zn(II) complex does not show any fluorescence emission. This rather unusual feature can be explained considering an electron transfer process involving the benzylic nitrogens.

Introduction

Chemosensors are molecules capable of binding a substrate and at the same time signaling its presence. One attractive method of signaling is the use of the fluorescence emission technique, because of its great sensitivity.^{1–9} In order to obtain a quantification of a fluorescence emission signal upon the binding of a receptor it is necessary to observe one of these

two cases: chelation enhancement of the fluorescence (CHEF) or chelation enhancement of quenching (CHEQ) effects. The first generation of chemosensors were constituted by aromatic heterocycles, for example those containing nitrogen or oxygen, in which both functions (binding and signaling) were attributed to the same part of the molecule, and for this reason they are called *intrinsic chemosensors* (Scheme 1). Among these, phenanthroline derivatives have received much attention in the past few years, due to the intense fluorescence emission of the phenanthroline unit as well as to the presence of two aromatic nitrogens which can act cooperatively in binding cations.¹⁰ In the second generation of chemosensors, *conjugate chemosensors*, the binding and signaling moieties are separated by a spacer and the two functions are ascribed to different moieties of the molecule, as shown in Scheme 1. Polyamine macrocycles are undoubtedly versatile receptors for metal cations.^{11–17} Depending on their structural features, they can form stable metal chelates in aqueous solution and/or act as selective complexant

[†] University of Florence.

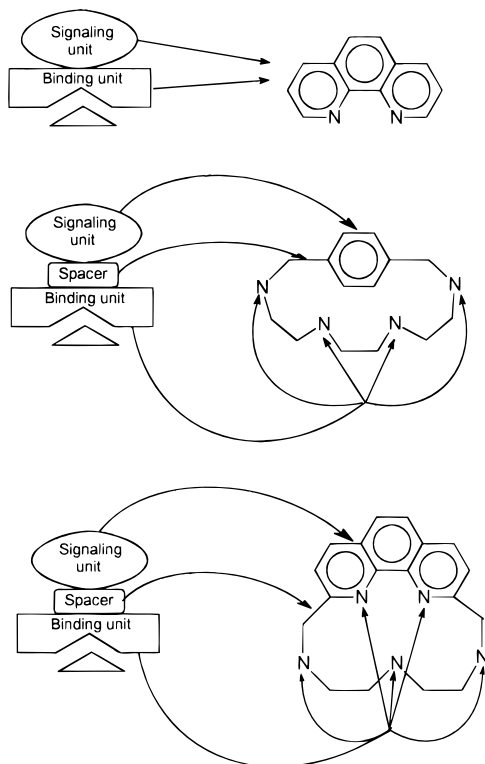
[‡] University of Urbino.

[§] Universidade Nova de Lisboa.

- (1) (a) Bissel, R. A.; De Silva, A. P.; Gunaratne, H. Q. N.; Lynch, P. L. M.; Maguire, G. E. M.; Sandanayake, K. R. A. S. *Chem. Soc. Rev.* **1992**, *21*, 187 (b) Bissel, R. A.; De Silva, A. P.; Gunaratne, H. Q. N.; Lynch, P. L. M.; McCoy, C. P. Maguire, G. E. M.; Sandanayake, K. R. A. S. *Top. Curr. Chem.* **1993**, *168*, 223. (c) De Silva, A. P.; Gunaratne, H. Q. N.; Gunnlaugsson, T.; Huxley, A. J.; McCoy, C. P.; Rademacher, J. T.; Rice, T. E. *Chem. Rev.* **1997**, *97*, 1515.
- (2) Balzani, V.; Scandola, F. *Supramolecular Photochemistry*; Horwood: Chichester, England, 1991.
- (3) (a) Czarnik, A. W., Ed. *Fluorescent Chemosensors for Ion and Molecule Recognition*; ACS Symposium Series 538; American Chemical Society: Washington, DC, 1992. (b) Huston, M. E.; Haider, K. W.; Czarnik, A. W. *J. Am. Chem. Soc.* **1988**, *110*, 4460.
- (4) (a) Fabrizzi, L.; Licchelli, M.; Pallavicini, P.; Perotti, A.; Taglietti, A.; Sacchi, D.; *Chem.—Eur. J.* **1996**, *1*, 75. (b) Fabrizzi, L.; Licchelli, M.; Pallavicini, P.; Taglietti, A. *Inorg. Chem.* **1996**, *35*, 1733.
- (5) (a) Sousa, L. R.; Larson, J. M. *J. Am. Chem. Soc.* **1977**, *99*, 307. (b) Larson, J. M.; Sousa, L. R. *J. Am. Chem. Soc.* **1978**, *100*, 1943.
- (6) Shizuka, H.; Takada, K.; Morita, T. *J. Phys. Chem.* **1980**, *84*, 994.
- (7) Bouas-Laurent, H.; Castellan, A.; Daney, M.; Desvergne, J.-P.; Guinand, G.; Marsau, P.; Riffaud, M.-H. *J. Am. Chem. Soc.* **1986**, *108*, 315.
- (8) Valeur, B.; Bourson, J.; Pouget, J.; Kaschke, M.; Nernsting, N. P. *J. Phys. Chem.* **1992**, *96*, 6545.

- (9) (a) Inoue, M. B.; Velazquez, E. F.; Medrano, F.; Ochoa, K. L.; Galvez, J. C.; Inoue, M.; Fernando, Q. *Inorg. Chem.* **1998**, *37*, 4070. (b) (a) Inoue, M. B.; Medrano, F.; Inoue, M.; Raitsimring, A.; Fernando, Q. *Inorg. Chem.* **1997**, *36*, 2335.
- (10) Sammes, P. G.; Yahioğlu, G. *Chem. Soc. Rev.* **1994**, *23*, 327 and references therein.
- (11) (a) Lindoy, L. F. *The Chemistry of Macrocyclic Ligand Complexes*; Cambridge University Press: Cambridge, U.K., 1989. (b) Lindoy, L. F. *Pure Appl. Chem.* **1997**, *69*, 2179.
- (12) (a) Bradshaw, J. S. *Aza-crown Macrocycles*; Wiley: New York, 1993. (b) Izatt, R. M.; Bradshaw, J. S.; Nielsen, S. A.; Lamb, J. D.; Christensen J. J.; Sen, D. *Chem. Rev.* **1985**, *85*, 271. (c) Izatt, R. M.; Pawlak, K.; Bradshaw, J. S.; Bruening, R. L. *Chem. Rev.* **1991**, *91*, 1721.

Scheme 1



agents for metal cations.^{11,12} For these reasons they are often chosen as metal-binding moieties in conjugate chemosensors. Recently, we reported the synthesis of a new series of polyamine macrocycles containing a phenanthroline unit as an integral part of the cyclic framework.¹⁷ The simplest of them, 2,5,8-triaza[9]-10,23-phenanthrolinephane (**L**), contains a triamine chain linking the 2,9-phenanthroline positions. Therefore, this system can be considered as an example of a combination of both *intrinsic* and *conjugate chemosensors*: while the polyamine unit is used exclusively for the function of binding, the phenanthroline unit can be used not only for signaling but also for binding.

In this paper we have analyzed the fluorescence emission of this chemosensor and the modulation of this property brought about by protonation and Zn(II) coordination.

Experimental Section

Ligand 2,5,8-triaza[9]-10,23-phenanthrolinephane (**L**) was prepared as previously reported.¹⁷

[H₃L]Br₃·H₂O. This compound can be obtained in almost quantitative yield by addition of 48% HBr to an ethanol solution of **L**. Anal. Calcd for C₁₈H₂₄Br₃N₅: C, 38.05; H, 4.61; N, 12.33. Found: C, 38.3;

- (13) (a) Lehn, J. M. *Angew. Chem., Int. Ed. Engl.* **1988**, *27*, 89. (b) Mertes, K. B.; Lehn, J. M. In *Comprehensive Coordination Chemistry*; Wilkinson, G., Ed.; Pergamon: Oxford, 1987; p 915. (c) Lehn, J. M. *Supramolecular Chemistry* VCH: New York, 1995.
- (14) Guerriero, P.; Tamburini, S.; Vigato, P. A. *Coord. Chem. Rev.* **1995**, *110*, 17.
- (15) Nelson, J.; McKee, V.; Morgan, G. In *Progress in Inorganic Chemistry*; Karlin, K. D., Ed.; Wiley: New York, 1998; Vol. 47, p 167.
- (16) (a) Bazzicalupi, C.; Bencini, A.; Bianchi, A.; Fusi, V.; Paoletti, P.; Valtancoli, B.; Zanchi, D. *Inorg. Chem.* **1997**, *36*, 2784. (b) Bencini, A.; Bianchi, A.; Paoletti, P.; Paoli, P. *Coord. Chem. Rev.* **1992**, *120*, 51. (c) Bencini, A.; Bianchi, A.; Paoletti, P.; Paoli, P. *Pure Appl. Chem.* **1993**, *65*, 381.
- (17) (a) Bazzicalupi, C.; Bencini, A.; Fusi, V.; Giorgi, C.; Paoletti, P.; Valtancoli, B. *Inorg. Chem.* **1998**, *37*, 941. (b) Bazzicalupi, C.; Bencini, A.; Fusi, V.; Giorgi, C.; Paoletti, P.; Valtancoli, B. *J. Chem. Soc., Dalton Trans.* **1999**, 393.

Table 1. Crystal Data and Structure Refinement for [H₃L]Br₃·H₂O (a) and for [ZnL(H₂O)](ClO₄)₂ (b)

	a	b
empirical formula	C ₁₈ H ₂₆ Br ₃ N ₅ O	C ₁₈ H ₂₅ Cl ₂ N ₅ O ₉ Zn
fw	568.17	589.68
temp, K	298	298
wavelength, Å	0.710 69	0.710 69
space group	<i>P</i> 2 ₁ / <i>c</i>	<i>P</i> 2 ₁ / <i>c</i>
unit cell dimens		
<i>a</i> , Å	13.750(6)	14.194(4)
<i>b</i> , Å	7.875(9)	11.959(4)
<i>c</i> , Å	20.487(9)	15.082(6)
β, deg	90.48(3)	114.90(2)
vol, Å ³	2218(3)	2322.1(14)
Z	4	4
density (calcd), Mg/m ³	1.701	1.687
abs coeff, mm ⁻¹	5.473	1.348
cryst size, mm	0.3 × 0.15 × 0.1	0.2 × 0.2 × 0.1
final <i>R</i> indices [<i>I</i> > 2σ(<i>I</i>)] ^a	R1 = 0.0655 wR2 = 0.1363	R1 = 0.0836 wR2 = 0.1961
<i>R</i> indices (all data) ^a	R1 = 0.1498 wR2 = 0.1840	R1 = 0.1552 wR2 = 0.2468

$$^a R1 = \frac{\sum ||F_o| - |F_c||}{\sum |F_o|}; wR2 = \frac{[\sum w(F_o^2 - F_c^2)^2 / \sum w F_o^4]^{1/2}}{\sum w F_o^2}$$

H, 4.5; N, 12.4. Crystals suitable for X-ray analysis were obtained by slow evaporation of an ethanol/water solution containing [H₃L]Br₃·H₂O.

[ZnL(H₂O)](ClO₄)₂. A solution of Zn(ClO₄)₂·6H₂O (3.7 mg, 0.01 mmol) in water (5 cm³) was slowly added to an aqueous solution (5 cm³) of [H₃L]Br₃ (5.5 mg, 0.01 mmol). The pH was adjusted to 7 with 0.1 M NaOH. To the resulting solution was added NaClO₄ (70 mg). Colorless crystals of the complex suitable for X-ray analysis were obtained by slow evaporation at room temperature of this solution. Yield: 5 mg (95%). Anal. Calcd for C₁₈H₂₅N₅Cl₂O₉Zn: C, 36.66; H, 3.93; N, 11.88. Found: C, 36.5; H, 4.0; N, 11.85. **CAUTION:** *Perchlorate salts of metal complexes with organic ligands are potentially explosive; these compounds must be handled with caution!*

X-ray Structure Analysis. Analyses on prismatic colorless single crystals of [H₃L](Br₃)·H₂O (**a**) and of [ZnL(H₂O)](ClO₄)₂ (**b**) were carried out with an Enraf-Nonius CAD4 X-ray diffractometer which uses an equatorial geometry. Graphite-monochromated Mo Kα radiation was used for cell parameter determinations and data collections. A summary of the crystallographic data is reported in Table 1.

Cell parameters for both compounds were determined by least-squares refinement of diffractometer setting angles for 25 carefully centered reflections. The intensities of two standard reflections per compound were monitored during data collections to check the stability of the diffractometer and of the crystal; no loss of intensity was recognized.

Totals of 3964 ($2\theta_{\max} = 50^\circ$) for **a** and 4234 ($2\theta_{\max} = 50^\circ$) for **b** were collected. Intensity data were corrected for Lorentz and polarization effects, and an absorption correction was applied once the structures were solved by the DIFABS method.¹⁸ (Compound **a**: φ and μ correction, max = 1.409 184, min = 0.818 711; θ corrections, max = 1.023 811, min = 0.835 253. Compound **b**: φ and μ correction, max = 1.227 609, min = 0.790 746; θ corrections, max = 1.036 124, min = 0.908 104.)

These structures were solved by direct methods of the SIR92 program.¹⁹ Refinements were performed by means of the full-matrix least-squares method of SHELXL-93²⁰ programs which uses the analytical approximation for the atomic scattering factors and anomalous dispersion corrections for all atoms from ref 21.

- (18) Walker, N.; Stuart, D. D. *Acta Crystallogr., Sect. A* **1983**, *39*, 158.
- (19) SIR 92: Altamore, A.; Casciarano, G.; Giacobozzo, C.; Guagliardi, A. *J. Appl. Crystallogr.* **1993**, *26*, 343.
- (20) Sheldrick, G. M. *SHELXS-93: Program for Crystal Structure Refinement*; Institut für Anorganische Chemie de Universität Göttingen: Göttingen, Germany.
- (21) *International Tables for X-ray Crystallography*; Kynoch Press: Birmingham, England, 1974; Vol. IV.

The function minimized was $\sum w(F_o^2 - F_c^2)^2$ with $w = 1/[\sigma^2(F_o^2) + (aP)^2 + bP]$ and $P = (F_o^2 + 2F_c^2)/3$, where a and b are refined parameters.

(a) **[H₃L]Br₃·H₂O**. Crystals of this compound belong to the monoclinic family, space group $P2_1/c$ ($Z = 4$), and lattice constants $a = 13.750(6)$ Å, $b = 7.875(9)$ Å, $c = 20.487(9)$ Å, $\beta = 90.48(3)^\circ$. All of the non-hydrogen atoms, except the oxygen atom belonging to the water solvent molecule, were anisotropically refined. The hydrogen atoms were introduced in calculated positions and their coordinates refined in agreement with those of the linked atoms. Overall refined temperature factors were used for hydrogen atoms belonging to the phenanthroline unit and to the aliphatic chain, respectively. The ΔF map, carried out in the last refinement step, did not allow the hydrogen atoms of the water molecule to be localized. The final agreement factors for 241 refined parameters were $R1 = 0.0655$ (for 1987 reflections with $I > 2\sigma(I)$) and $wR2 = 0.1840$ (for all data).

(b) **[ZnL(H₂O)](ClO₄)₂**. Crystals of this compound belong to the monoclinic family, space group $P2_1/c$ ($Z = 4$), and lattice constants $a = 14.194(4)$ Å, $b = 11.959(4)$ Å, $c = 15.082(6)$ Å, $\beta = 114.90(2)^\circ$. Double positions introduced with population parameters 0.6 and 0.4 were found in the ethylenic chains of the macrocycle for C14, C15, C16' and C14', C15', C16, respectively.

All of the non-hydrogen atoms were anisotropically refined, except the carbon atoms in double position (C14, C14', C15, C15', C16, and C16'). The hydrogen atoms were introduced in calculated positions and their coordinates refined in agreement with those of the linked atoms. Those hydrogen atoms which should have been introduced in double position were omitted. Overall refined temperature factors were used for hydrogen atoms belonging to the phenanthroline unit and to the aliphatic chain, respectively. Rotational disorder, giving rise to high thermal parameters for the oxygen atoms, was found for the perchlorate anions. The ΔF map, carried out in the last refinement step, allowed the water hydrogen atoms, which were introduced in the calculation and isotropically refined, to be localized. The final agreement factors for 324 refined parameters were $R1 = 0.0836$ (for 2250 reflections with $I > 2\sigma(I)$) and $wR2 = 0.2468$ (all data).

Potentiometric Measurements. Equilibrium constants for protonation and complexation reactions with **L** were determined by potentiometric measurements ($\text{pH} = -\log [\text{H}^+]$) in 0.1 mol dm⁻³ NMe₄Cl at 298.1 ± 0.1 K, by using the potentiometric equipment that has been already described.²² The combined glass electrode was calibrated as a hydrogen concentration probe by titrating known amounts of HCl with CO₂-free NaOH solutions and determining the equivalent point by Gran's method,²³ which allows determination of the standard potential E° , and the ionic product of water ($\text{p}K_w = 13.83(1)$) at 298.1 K in 0.1 mol dm⁻³ NMe₄Cl. Ligand and metal ion concentrations in the range 1×10^{-3} to 2×10^{-3} mol dm⁻³ were employed in the potentiometric measurements; three titration experiments (about 100 data points each) were performed in the pH ranges 2.5–10.5. The computer program HYPERQUAD²⁴ was used to calculate equilibrium constants from emf data. All titrations were treated either as single sets or as separated entities, for each system, without significant variation in the values of the determined constants.

NMR Spectroscopy. ¹H (200.0 MHz) and ¹³C NMR (50.32 MHz) spectra in D₂O solutions at different pH values were recorded at 298 K in a Bruker AC-200 spectrometer. In ¹H NMR spectra peak positions are reported relative to HOD at 4.75 ppm. Dioxane was used as reference standard in ¹³C NMR spectra ($\delta = 67.4$ ppm). ¹H–¹H and ¹H–¹³C 2D correlation experiments were performed to assign the signals. Small amounts of 0.01 mol dm⁻³ NaOD or DCl solutions were added to a solution of the ligand to adjust the pD. The pH was calculated from the measured pD values using the following relationship:²⁵

$$\text{pH} = \text{pD} - 0.40$$

Spectrophotometric and Spectrofluorimetric Titrations. Absorption spectra were recorded on a Perkin-Elmer Lambda 6 spectrophotometer, and fluorescence emission was recorded on a SPEX F111 Fluorolog spectrofluorimeter. HCl and NMe₄OH were used to adjust the pH values, which were measured on a Metrohm 713 pH meter.

Results and Discussion

Protonation. Crystal Structure of of [H₃L](Br)₃·H₂O. The crystal structure consists of triprotonated ligand [H₃L]³⁺, bromide anions, and water solvent molecules. An ORTEP²⁶ drawing of [H₃L]³⁺ with atom labeling is depicted in Figure 1a.

The macrocycles adopts a bent conformation; the phenanthroline unit and the benzylic nitrogens N3 and N5, i.e., the aliphatic nitrogens adjacent to phenanthroline, are almost coplanar (maximum deviation 0.279(9) Å for N3). This plane is almost perpendicular to the plane formed by the N3, N4, and N5 amine groups, their dihedral angle being 104.1(3)°. Moreover, the N3, N4, and N5 amine groups of the aliphatic chain are in the *endo* conformation. Consequently, several hydrogen bonds are formed inside the macrocyclic cavity. The H4A hydrogen atom, linked to the central amine group, points inside the macrocyclic cavity, giving rise to H-bond interactions with the phenanthroline nitrogens N1 and N2 (N4···N1 3.11(1) Å, N4···N2 2.86(1) Å). The H3A and H5B hydrogens are also partially enclosed in the ligand cavity, giving rise to intramolecular H-bonds with the phenanthroline nitrogens (N3···N2 2.75(1) Å and N5···N1 2.67(1) Å). Hydrogen bond interactions are also observed between N3, N4, and N5 and the bromide anions. (N3···Br2 ($-x + 1, -y + 1, -z + 2$) 3.276(8) Å, N5···Br2 ($-x + 1, -y + 1, -z + 2$) 3.287(9) Å, N3···Br1 ($x - 1, y - 1, z$) 3.196(9) Å, N4···Br3 ($-x + 1, 0.5 + y, 1.5 - z$) 3.138(8) Å, N5···Br1 ($-x + 1, -y + 2, -z + 2$) 3.259(8) Å).

It is of interest to compare the structure of this cation with that of the triprotonated macrocycle [H₃D33]³⁺, recently reported by Altava et al.²⁷ In the triaza[11]paracyclophane D33, a triamine chain, similar to that of **L**, links the 1,4 positions of a durene moiety (Figure 1b). In [H₃D33]³⁺ the three acidic protons are located on the aliphatic nitrogens, which are in the *exo* conformation, and the macrocycle assumes an overall open conformation, which allows the minimization of the electrostatic repulsion between the charged polyammonium groups. As a matter of fact, although D33 contains an aromatic spacer smaller than **L**, the distance between the benzylic nitrogens in [H₃D33]³⁺ is remarkably larger than in [H₃L]³⁺ (6.85 Å vs 5.18 Å). Furthermore, in [H₃D33]³⁺ the benzylic nitrogens are located ca. 1.45 Å above the plane defined by the aromatic ring, while in [H₃L]³⁺ the benzylic nitrogens N3 and N5 (Figure 1a) are coplanar and close to the phenanthroline unit. In [H₃L]³⁺ the particular folded conformation is accompanied by a severe stress of the aliphatic chain, as evidenced by the values of the C–C–N and C–N–C bond angles, which present significant deviations from the sp³ theoretical ones. The strained structure of [H₃L]³⁺ can be ascribed to the stiffening of the macrocyclic framework determined by the presence of a large and rigid aromatic moiety in a rather small cyclic molecule as well as by the short ethylenic chains connecting the amine groups.

Solution Studies. The protonation equilibria of **L** have been studied by means of potentiometric measurements in aqueous

(22) Bianchi, A.; Bologni, L.; Dapporto, P.; Micheloni, M.; Paoletti, P. *Inorg. Chem.* **1984**, *23*, 1201.

(23) (a) Gran, G. *Analyst (London)* **1952**, *77*, 661. (b) Rossotti, F. J.; Rossotti, H. J. *J. Chem. Educ.* **1965**, *42*, 375.

(24) Gans, P.; Sabatini, A.; Vacca, A. *J. Chem. Soc., Dalton Trans.* **1985**, 1195–1200.

(25) Covington, A. K.; Paabo, M.; Robinson, R. A.; Bates, R. G. *Anal. Chem.* **1968**, *40*, 700.

(26) Johnson, C. K. ORTEP. Report ORNL-3794; Oak Ridge National Laboratory: Oak Ridge, TN, 1971.

(27) Altava, B.; Bianchi, A.; Bazzicalupi, C.; Burguete, M. I.; Garcia-España, E.; Luis, S. V.; Miravet, J. F. *Supramol. Chem.* **1997**, *8*, 287.

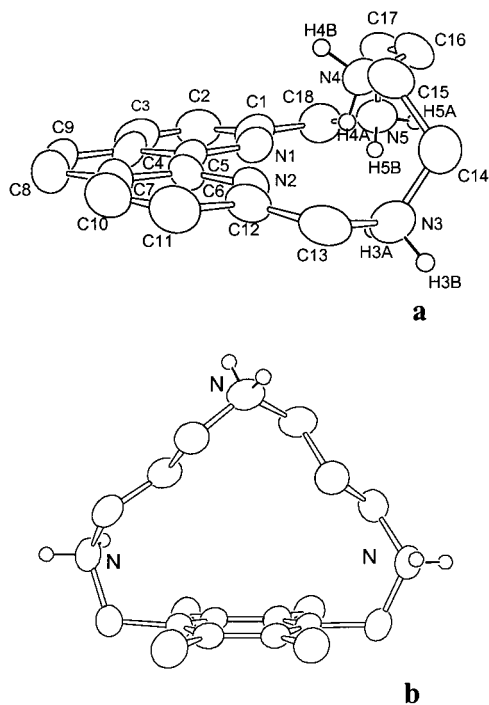


Figure 1. ORTEP drawings of $[H_3L]^{3+}$ (a) and of $[H_3D33]^{3+}$ (b).²⁷

Table 2. Logarithms of the Equilibrium Constants Determined in $0.1 \text{ mol dm}^{-3} \text{ NMe}_4\text{Cl}$ at 298.1 K for H^+ and Zn^{2+} Binding by **L**

	log <i>K</i>
$L + H^+ = [HL]^+$	9.99(1)
$[HL]^+ + H^+ = [H_2L]^{2+}$	7.72(1)
$[H_2L]^{2+} + H^+ = [H_3L]^{3+}$	4.11(1)
$Zn^{2+} + L = [ZnL]^{2+}$	16.15(2)
$[ZnL]^{2+} + OH^- = [ZnLOH]^+$	4.44(6)
$[ZnLOH]^+ + OH^- = [ZnL(OH)_2]$	2.75(8)

solution ($0.1 \text{ mol dm}^{-3} \text{ NMe}_4\text{Cl}$, 298.1 K), and the results are reported in Table 2, together with the stability constants of the Zn(II) complexes. As can be seen, **L** can bind up to three protons in aqueous solutions. Since phenanthroline nitrogens are characterized by far lower basicity than amine nitrogens, it is expected that protonation of **L** takes place on the polyamine chain. This hypothesis is confirmed by the analysis of the absorption spectra recorded on solutions containing **L** at various pH values. Figure 2 shows the pH dependence of the absorption spectra of the chemosensor. Two different spectral modifications can be observed upon protonation: (i) a very small red shift from pH 4.72 to 1 (Figure 2b) and (ii) a small blue shift from basic to moderately acidic pH's (Figure 2c). Significant red shifts upon protonation have been reported²⁸ in the case of systems containing the chromophore 1,10-phenanthroline but not bearing amine groups. Although protonation occurs on the nitrogens of the polyaza chain, some hydrogen bond interactions with the nitrogens of the phenanthroline take place. This effect can also be observed in the inset of Figure 2a, where, depending on pH, small differences of the absorbance are shown. The largest variations occur upon removal of the first and second protons

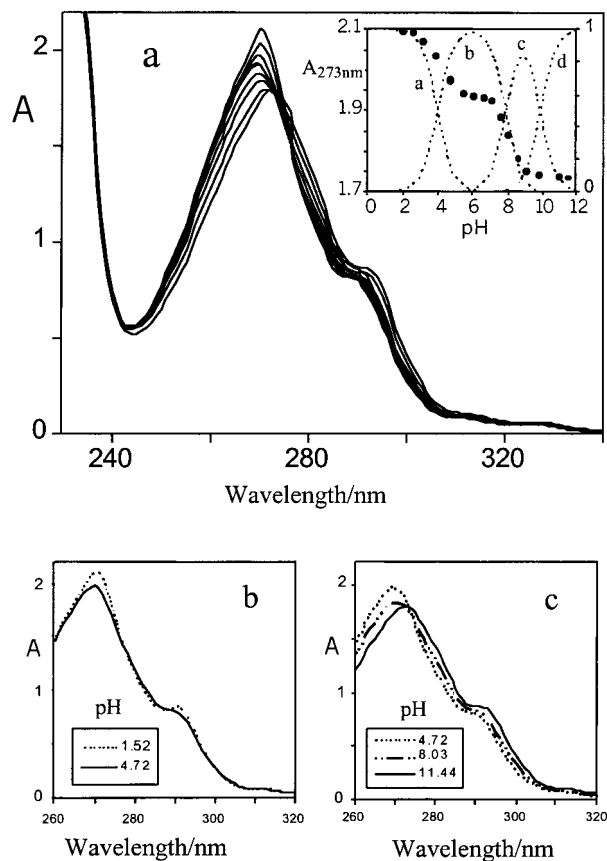


Figure 2. (a) pH dependence of the absorption spectra of **L** ($[L] = 5 \times 10^{-5} \text{ M}$, $I = 0.15 \text{ M}$): pH 1.52, 3.89, 4.72, 6.65, 7.06, 7.64, 8.03, 8.66, 11.74. Inset: Adsorbance at 270 nm (●) and molar fractions of the protonated forms of **L** (dashed lines, a = $[H_3L]^{3+}$, b = $[H_2L]^{2+}$, c = $[HL]^+$, d = **L**) as a function of pH. (b) Absorption spectra at acidic pH's. (c) Absorption spectra from neutral to alkaline.

from the triprotonated $[H_3L]^{3+}$ species, suggesting that in the fully protonated as well as in the diprotonated form the protons of the aliphatic NH_2^+ groups give hydrogen bond interactions with the phenanthroline nitrogens, as actually observed in the crystal structure of the $[H_3L]^{3+}$ cation.

The protonation pattern of **L** has been clarified by recording 1H and ^{13}C NMR spectra in aqueous solution at different pH values. The ^{13}C spectrum of **L** at pH 12.0, where the unprotonated amine predominates in solution, exhibits nine peaks, three for the aliphatic carbons C1, C2, and C3 (at 48.4, 49.0, and 52.9 ppm, respectively) and six for the aromatic carbons C4–C9. The 1H spectrum of **L** at this pH shows two multiplets at 2.48 and 2.58 ppm (attributed to the protons H1 and H2 of the ethylenic chain), a singlet at 4.0 ppm (the aliphatic proton H3), two doublets at 7.43 and 8.02 (H5 and H6), and a singlet at 7.40 ppm (H9). These spectral features indicate a C_{2v} time-averaged symmetry. This symmetry is preserved throughout all the pH range investigated. Figure 3 shows the 1H NMR chemical shifts of **L** as a function of pH. In the pH range 12–9, where the first proton binds to the ligand, the signal of the hydrogen H1, in the α -position with respect to N1, exhibits a marked downfield shift, while the other signals do not shift appreciably. This strongly suggests that in the $[HL]^+$ species the acidic proton is located on the central amine group N1, as drawn in Scheme 2. In the pH range 9–6.5, where the diprotonated $[H_2L]^{2+}$ species is formed, the resonances of the protons H2 and H3, adjacent to N2, bear a remarkable downfield shift, while an upfield shift is observed for the H1 signal. These spectral

(28) (a) Armaroli, N.; De Cola, L.; Balzani, V.; Sauvage, J.-P.; Dietrich-Buchecker, C. O.; Kern, J. M. *J. Chem. Soc., Faraday Trans.* **1992**, 88, 553. (b) Kern, J. M.; Sauvage, J.-P.; Weidmann, J. L.; Armaroli, N.; Flamigni, L.; Ceroni, P.; Balzani, V. *Inorg. Chem.* **1997**, 36, 5329. (c) Armaroli, N.; De Cola, L.; Balzani, V.; Sauvage, J.-P.; Dietrich-Buchecker, C. O.; Kern, J. M.; Bailal, A. *J. Chem. Soc., Dalton Trans.* **1993**, 3241. (d) Armaroli, N.; Ceroni, P.; Balzani, V.; Kern, J. M.; Sauvage, J.-P.; Weidmann, J. L. *J. Chem. Soc., Faraday Trans.* **1997**, 93, 4145.

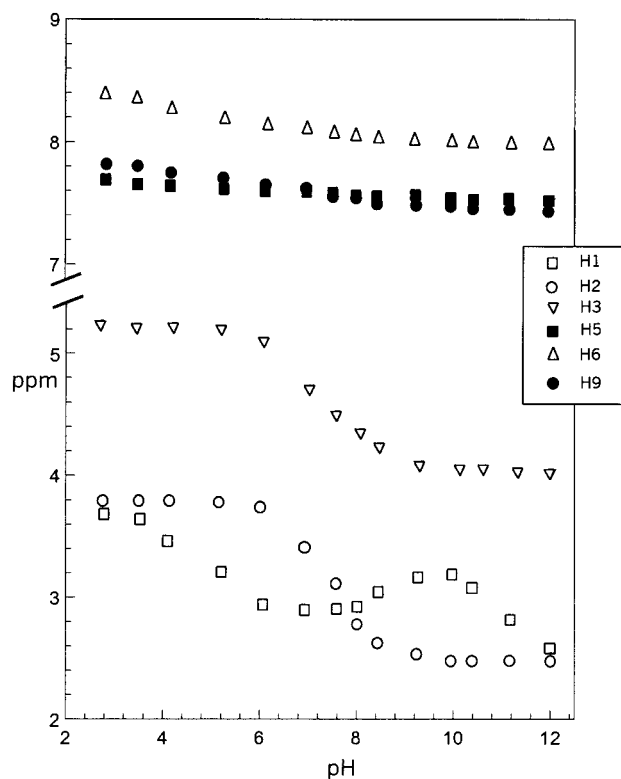
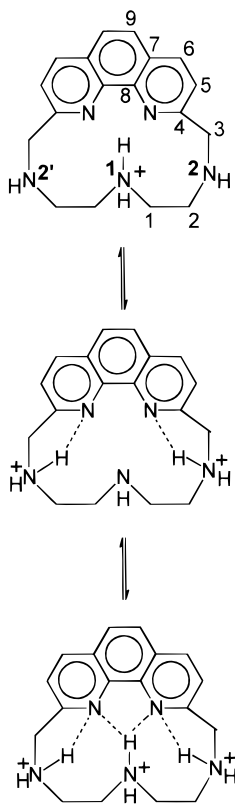


Figure 3. Experimental ^1H chemical shifts of **L** as a function of pH.

Scheme 2



features indicate that the second protonation step gives rise to a reorganization in the proton distribution, i.e., in $[\text{H}_2\text{L}]^{2+}$ both of the acidic protons are localized on the benzylic N2 and N2' nitrogens, while N1 remains unprotonated. This evidence is confirmed by the ^{13}C spectra recorded in the same pH range, which show that the resonances of the carbon atoms C1 and

C4, in the β -position with respect to N2, shift upfield, in good agreement with the β -shift reported for protonation of polyamines.²⁹ Such a disposition of the protons in the $[\text{H}_2\text{L}]^{2+}$ species would mean a minimum in electrostatic repulsions, since the protons occupy alternate positions, separated from each other by the unprotonated N1 nitrogen and by the aromatic systems.

Finally, at more acidic pH's, the third protonation step occurs on the central N1 amine group, as evidenced by a downfield shift of the H1 signal in the pH range 6–2. It is to be noted that the resonances of the aromatic protons do not exhibit significant changes in their chemical shifts throughout the pH range investigated, indicating that the acidic protons are mostly located on the amine groups. The slight downfield shift observed for the resonances of the aromatic protons H6 and H9 at acidic pH's indicate a partial involvement of the aromatic nitrogens in the stabilization of the highly protonated species. As a matter of fact, as shown by the crystal structure of $[\text{H}_3\text{L}]^{3+}$, the phenanthroline nitrogens are strongly involved in a hydrogen bond network with the polyammonium groups of the aliphatic chain. On the other hand, a partial localization of protons on the heteroaromatic nitrogens cannot be excluded.

In contrast with absorption, the fluorescence emission is very dependent on the protonation state of the receptor unit. Independently of pH, the shape and position of the fluorescence emission spectra of **L** are identical to those of phenanthroline. The absence of lower energy fluorescence emission bands, which are usually observed in protonated phenanthroline systems not bearing amine groups, is to be noted.²⁸ This observation suggests, once more, that in the bi- and triprotonated species of the macrocycle the phenanthroline nitrogens are not protonated but only involved in weak hydrogen-bonding interactions with the protonated amine groups.

The inset of Figure 4a clearly shows that the intensity of the emission decreases dramatically with increasing pH from neutral to alkaline pH's. On the other hand, a slight decreasing of the emission intensity is also observed at acidic pH's (pH < 5). As shown in the inset of Figure 4a, the fully protonated form of **L** is not the most emissive species. This is one interesting consequence of the "dual nature" of this chemosensor. In effect for the fully protonated form of the chemosensor, as well as for the diprotonated one, the signaling phenanthroline unit is partially involved in protonation, due to the hydrogen bond interactions between NH_2^+ groups and the aromatic nitrogens. We know that, in the parent compound phenanthroline, protonation also decreases substantially the intensity of the fluorescence emission, because the $^1n\pi^* \rightarrow \text{gs}$ transition is stabilized with respect to the $\pi\pi^* \rightarrow \text{gs}$ one. The same type of argument would in principle be used to explain the dramatic quenching effect observed in the pH region between 7.64 and 8.66; upon protonation of the aliphatic amine groups the $^1n\pi^* \rightarrow \text{gs}$ state would be pushed up, leaving the $^1\pi\pi^* \rightarrow \text{gs}$ as the lowest transition. However, the shifts observed in the absorption bands suggest that upon protonation the $\pi\pi^* \rightarrow \text{gs}$ state becomes slightly unstable.

An alternative explanation to this effect could be an intramolecular electron transfer from the unprotonated amine groups to the excited phenanthroline. This process is thermodynamically favorable by -0.46 eV ³⁰ and was found in many other similar

(29) (a) Batchelor, J. C.; Prestegard, J. H.; Cushley, R. J.; Lipsy, S. R. *J. Am. Chem. Soc.* **1973**, *95*, 6558. (b) Quirt, A. R.; Lyster, J. R.; Peat, I. R.; Cohen, J. S.; Reynold, W. R.; Freedman, M. F. *J. Am. Chem. Soc.* **1974**, *96*, 570. (c) Batchelor, J. C. *J. Am. Chem. Soc.* **1975**, *97*, 3410. (d) Sarnesky, J. E.; Surprenant, H. L.; Molen, F. K.; Reilley, C. N. *Anal. Chem.* **1975**, *47*, 2116.

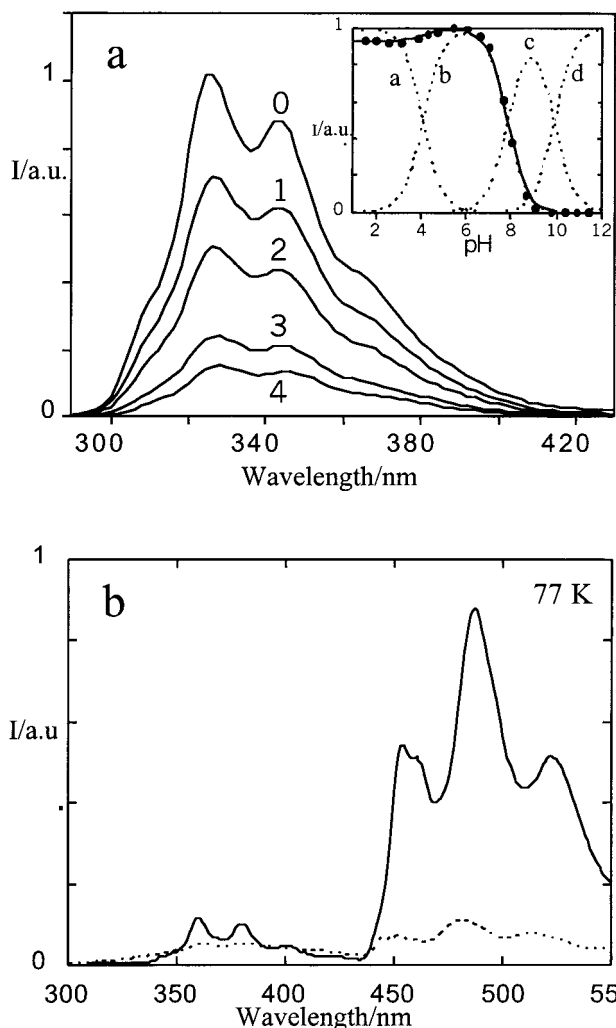


Figure 4. (a) Fluorescence emission spectra at different pH's (0, pH = 1.52; 1, pH = 7.64; 2, pH = 8.03; 3, pH = 8.66; 4, pH 9.78). Inset: Fluorescence emission (●) of **L** and molar fractions of the protonated forms of **L** (○) as a function of pH ($[L] = 2 \times 10^{-5}$ M; $I = 0.15$ M). (b) Fluorescence and phosphorescence emission spectra of $[H_3L]^{3+}$ (—) and of **L** (---) at 77 K (9:1 ethanol/methanol rigid matrix).

systems.³¹ In order to get more insight, luminescence measurements at 77 K were carried out in a 9:1 ethanol/methanol rigid matrix. The protonated form of **L** shows an intense phosphorescence emission (lifetime 2.0 s), as shown in Figure 4b. In contrast the unprotonated form exhibits a weak phosphorescence emission (lifetime 2.4 s), with intensity ca. 10-fold lower. This result is compatible with a decrease in the yield of intersystem crossing motivated by the electron transfer process that quenches the singlet state.

In conclusion, the largest fluorescence emission intensity is observed upon removal of the first proton from the central N1 atom, because of the following opposite effects: (i) the hydrogen bond interaction of phenanthroline nitrogens with the N1

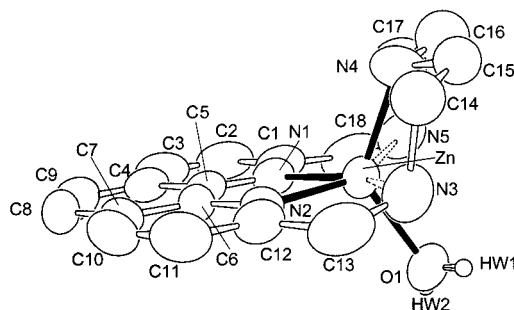


Figure 5. ORTEP drawing of the $[ZnL(H_2O)]^{2+}$ cation.

ammonium group, observed in the crystal structure of the $[H_3L]^{3+}$ cation, disappears, and thus the emission is expected to increase; (ii) however, the deprotonated central nitrogen is now available to quench the excited state centered at the phenanthroline unit, as shown in Scheme 2. In the present chemosensor the central nitrogen atom is not very efficient to quench the excited fluorophore, as for example when compared with analogous nitrogens of polyazacyclophanes.^{31c,32} The final balance of these two effects is a slight increase of the intensity of the fluorescence emission upon deprotonation of the $[H_3L]^{3+}$ to give the diprotonated $[H_2L]^{2+}$ cation, which is the most emissive species. The most dramatic variation occurs by removal of the second proton from the benzylic nitrogens N2 and N2', i.e., from the aliphatic nitrogens adjacent to phenanthroline (Scheme 2), to give the monoprotonated $[HL]^+$ cation. As previously discussed, in $[HL]^+$ the acidic proton is located on the N1 nitrogen and therefore both benzylic amine groups N2 and N2' are now available to the electron transfer quenching process. In conclusion the experimental results show that the benzylic nitrogens N2 and N2' are more efficient quenchers than the central nitrogen atom. This is exactly the opposite behavior than in the case of polyazacyclophane macrocyclic receptors.^{31c,32}

The comparison between the crystal structure of the phenanthroline-cyclophane $[H_3L]^{3+}$ and that of the polyazacyclophane $[H_3D33]^{3+}$ cations may suggest an explanation to this apparent contradiction. As previously discussed, in $[H_3D33]^{3+}$ both of the benzylic amine groups are in the *exo* conformation, while in $[H_3L]^{3+}$ the amine groups are in the *endo* conformation. Furthermore, in $[H_3L]^{3+}$ both the benzylic nitrogens N2 and N2' are close to the fluorophore. This suggests that the benzylic nitrogens of **L** are much more available for the quenching process than those of D33.

Zn(II) Coordination. Crystal Structure of the $[ZnL(H_2O)](ClO_4)_2$ Complex. The molecular structure consists of $[ZnL(H_2O)]^{2+}$ complex cations and perchlorate anions. An ORTEP²⁴ drawing of $[ZnL(H_2O)]^{2+}$ is shown in Figure 5, and selected bond distances and angles are reported in Table 3. The coordination geometry around the metal atom can be described as a distorted tetrahedron, whose vertexes are occupied by the phenanthroline nitrogens N1 and N2, the central aliphatic nitrogen N4, and a water molecule (O1). However, the Zn^{2+} forms two long bonds with the benzylic nitrogens N3 and N5 ($N3-Zn$ 2.460(8) Å, $N5-Zn$ 2.512(10) Å) to achieve pseudoprismatic geometry, the bases of the prism being defined by N2, N3, N4 and N1, O1, N5, respectively.

The macrocyclic framework adopts an overall conformation very similar to that found in the $[H_3L]^{3+}$ cation. Once again all three amine groups are in the *endo* conformation, with the

(30) Calculated from the oxidation potential of the model compound triethylamine (1.15 eV vs SCE), the redox potential of phenanthroline (-2.05 eV vs SCE), and the energy of the first singlet of phenanthroline (353 kJ mol⁻¹): Murov, S. L.; Carmichael, I.; Hug, G. L. *Handbook of Photochemistry*; Marcel Dekker: New York.

(31) (a) Bergonzi, R.; Fabbrizzi, L.; Licchelli, M.; Mangano, C. *Coord. Chem. Rev.* **1998**, *170*, 31. (b) De Silva, A. P.; Rupasinghe, R. A. D. *Chem. Commun. (Cambridge)* **1996**, 1660. (c) Bernardo, M. A.; Guerrero, J. A.; Garcia-España, E.; Luis, S. V.; Llinares, J. M.; Pina, F.; Ramirez, J. A.; Soriano, C. *J. Chem. Soc., Perkin Trans 2* **1996**, 2335.

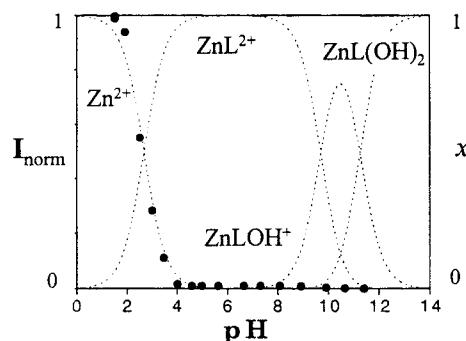
(32) Bernardo, M. A.; Parola, A. J.; Pina, F.; Garcia-España, E.; Marcelino, V.; Luis, S. V.; Miravet, J. F. *J. Chem. Soc., Dalton Trans.* **1995**, 993.

Table 3. Selected Bond Lengths (Å) and Angles (deg) for [ZnL(H₂O)](ClO₄)₂

Zn–O1	2.034(8)
Zn–N4	2.075(9)
Zn–N2	2.118(7)
Zn–N1	2.145(7)
Zn–N3	2.460(8)
Zn–N5	2.512(10)
O1–Zn–N4	125.5(4)
O1–Zn–N2	112.1(3)
N4–Zn–N2	110.3(4)
O1–Zn–N1	110.6(4)
N4–Zn–N1	111.2(3)
N2–Zn–N1	76.6(3)
O1–Zn–N3	83.2(4)
N4–Zn–N3	79.0(4)
N2–Zn–N3	71.8(3)
N1–Zn–N3	148.4(3)
O1–Zn–N5	85.9(4)
N4–Zn–N5	77.8(4)
N2–Zn–N5	145.5(3)
N1–Zn–N5	69.4(4)
N3–Zn–N5	141.6(4)

benzylic nitrogens N3 and N5 almost coplanar to the heteroaromatic unit (Figure 5). The ligand assumes a folded conformation with an angle of 93.0(5)° between the plane defined by the phenanthroline unit and the benzylic nitrogens (maximum deviation 0.20(1) Å for N5) and that formed by the amine groups N3, N4, and N5. As already observed in [H₃L]³⁺, the values of the C–C–N and C–N–C bond angles for the aliphatic chain indicate that this part of the ligand is remarkably strained. The similar conformational features of the macrocycle in [H₃L]³⁺ and in its Zn(II) complex further confirm that the insertion of the phenanthroline unit as an integral part of a rather small cyclic framework leads to a highly rigid macrocycle.

Solution Studies. Zn(II) coordination by **L** was studied by means of potentiometric measurements in 0.1 mol dm⁻³ NMe₄-Cl aqueous solution at 298.1 K. The species formed and the corresponding stability constants are reported in Table 2. It can be of interest to compare the stability constant of the present complex with that of the Zn(II) complex with the macrocyclic ligand 1,4,7,10,13-pentaazacyclopentadecane (**L1**),³³ which contains five secondary amine groups linked by ethylenic chains. For the [ZnL]²⁺ complex it was found that all five donors are involved in metal coordination. The formation constant of the **L** complex is by far lower than the **L1** one (log *K* = 16.15 for [ZnL]²⁺, Table 2, vs log *K* = 19.1 for [ZnL1]²⁺). Furthermore, the [ZnL]²⁺ complex gives hydroxylated species even at slightly alkaline pH's; on the contrary the **L1** complex does not display any tendency to form hydroxylated species. These different characteristic of the **L** and **L1** complexes may indicate that in the [ZnL]²⁺ complex some nitrogen donors are not bound, or are weakly bound to the metal. This suggestion is confirmed by the crystal structure of the [ZnL(H₂O)]²⁺ cation, which shows a rather distorted coordination environment for the Zn(II) ion, with both of the benzylic nitrogens weakly involved in metal coordination. These structural features can be ascribed to both steric and electronic factors due to the presence of a phenanthroline moiety in the cyclic framework. Phenanthroline is rigid, and therefore its insertion as an integral part of a polyamine macrocycle leads to a marked stiffening of the framework. Such a molecular rigidity may preclude the simultaneous participation of all of the amine nitrogens in the coordination to the metal cation. A similar effect has been already observed in polyaza-

**Figure 6.** Fluorescence emission (●) of **L** in the presence of Zn(II) (1:1 molar ratio) and molar fractions of the Zn(II) complexes with **L** (···) as a function of pH ([**L**] = 2 × 10⁻⁵ M; *I* = 0.15 M).

cyclophanes containing a benzene in the macrocyclic ring.³⁴ Furthermore, phenanthroline has electron-withdrawing properties, which reduce the basicity and the donor ability of the benzylic amine groups adjacent to the heteroaromatic moiety. These characteristics make these amine groups less available for metal coordination and lead to an unsaturated coordination environment of Zn(II). As a consequence, water molecules can be bound at the free binding sites of the metal, as actually shown by the crystal structure of the [ZnL(H₂O)]²⁺ complex. Facile deprotonation of the coordinated water gives the [ZnLOH]⁺ hydroxo complex in aqueous solutions at slightly alkaline pH's; a dihydroxo species [ZnL(OH)₂] is also observed in strongly alkaline solutions. The structural characteristics described above strongly affect the fluorescence emission features of this Zn(II) complex. Zn(II) coordination usually gives a marked CHEF effect; the increased fluorescence emission intensity (CHEF effect) of *conjugate chemosensors*, brought about by Zn(II) coordination, has been described for several families of these molecules.¹⁻⁴ In principle, coordination of a positive substrate, such as proton or metal cations, to the amine nitrogens should prevent the electron transfer quenching process, merely by Coulombic effects. However, not all cations exhibit a CHEF effect. For example, Cu²⁺ or Ni²⁺ coordination gives rise to a CHEQ effect.³²

Figure 6 depicts the fluorescence emission titration curve of **L** in the presence of equimolar quantities of Zn²⁺. Figure 6 clearly shows that coordination of Zn(II) gives rise to an efficient quenching process of the fluorescence emission of phenanthroline. However, we verified that coordination of Zn(II) directly to free phenanthroline does not give any quenching effect.

The unexpected absence of emission of the zinc complex at room temperature can be rationalized considering the particular structural characteristics of ligand **L** and of its Zn(II) complex. According to the structure of the [ZnL(H₂O)]²⁺ cation, both of the benzylic amine groups (N3 and N5 in Figure 5) are weakly involved in metal coordination. These nitrogens are coplanar and close to the fluorophore. In addition, no protonated forms of the Zn(II) complex were detected by potentiometry. Therefore, in [ZnL]²⁺ the lone pairs of the benzylic nitrogens are available for the quenching process. On this basis the lack of fluorescence emission in this Zn(II) complex can probably be explained by an electron transfer process involving these nitrogens. An alternative to this mechanism, based on the influence of the complexation in the triplet state, can be considered. Two possible triplet states (³ππ* → gs on phenanthroline and ³CT → gs between the amine groups and phenanthroline) could arise upon complexation with the metal. The

(33) Kodama, E.; Kimura, E. *J. Chem. Soc., Dalton Trans.* **1978**, 1081.(34) Garcia-España, E.; Luis, S. V. *Supramol. Chem.* **1996**, 6, 257.

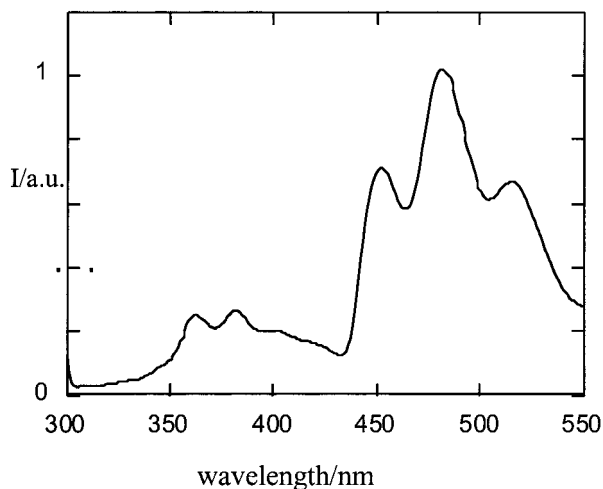


Figure 7. Fluorescence and phosphorescence emission spectra of the Zn(II) complex with **L** in a 9:1 ethanol/methanol rigid matrix. ($[\text{ZnL}]^{2+} = 2 \times 10^{-5}$).

emission spectrum recorded at 77 K in an ethanol-methanol 9:1 rigid matrix (Figure 7) shows that the Zn(II) complex with **L** exhibits in these conditions fluorescence and phosphorescence emission (lifetime 3.6 s). At room temperature, the triplet states could give a radiationless pathway, through the solvent sphere. Although this mechanism cannot be discharged, the fact that the Zn(II) complex with phenanthroline possessing an identical triplet state is emissive at room temperature may give confidence

to a mechanism involving an electron transfer process involving the benzylic amine groups.

Concluding Remarks. The connection of the 2,9 positions of phenanthroline, a large and rigid aromatic unit, with a short triamine chain gives rise to a stiffened macrocyclic structure. As a consequence of these structural characteristics, both of the benzylic nitrogens of the chemosensor **L** are in the *endo* conformation and close to phenanthroline. Therefore, these amine groups may act as effective quenchers of the fluorescence emission of phenanthroline. In the Zn(II) complex the metal is bound through the heteroaromatic moiety. The rigid macrocyclic framework does not allow the simultaneous formation of strong covalent bonds between the metal and the benzylic nitrogens. This structure suggests that the unexpected lack of fluorescence of the Zn(II) complex is due to the benzylic nitrogen lone pairs, which are available for the quenching process.

Acknowledgment. Financial support by the Italian Ministero dell'Università e della Ricerca Scientifica e Tecnologica (quota 40%) and by Italian Research Council (CNR) is gratefully acknowledged. M.A.B. thanks Fundação para a ciência e Tecnologia (Grant PRAXIS XXI/BD/4504/94).

Supporting Information Available: Tables of crystallographic and experimental data, complete atomic positional parameters, anisotropic temperature factors, and bond distances and angles for $[\text{H}_3\text{L}](\text{Br})_3 \cdot \text{H}_2\text{O}$ and $[\text{ZnL}(\text{H}_2\text{O})](\text{ClO}_4)_2$. This material is available free of charge via the Internet at <http://pubs.acs.org>.

IC981374K